Modeling and propagating inventory-based sampling uncertainty in the large-scale forest demographic model "MARGOT"

Timothée Audinot, Holger H. Wernsdorfer, Gilles Le Moguédec, Jean-Daniel Bontemps

Received: 26 November 2021 | Accepted: 28 June 2022

DOI: 10.1111/nrm.12352

Natural Resource Modeling WILEY

Modeling and propagating inventory-based sampling uncertainty in the large-scale forest demographic model "MARGOT"

Timothée Audinot[1,2,3] | **Holger Wernsdörfer**[2] | **Gilles Le Moguédec**[4] | **Jean-Daniel Bontemps**[1]

[1]IGN, Laboratoire d'Inventaire Forestier (LIF), Nancy, France

[2]Université de Lorraine, AgroParisTech, INRAE, SILVA, Nancy, France

[3]Université Gustave Eiffel, ENSG, IGN, Marne-la-Vallée, France

[4]AMAP, Université Montpellier, INRAE, Cirad CNRS, IRD, Montpellier, France

Correspondence
Timothée Audinot, IGN, Laboratoire d'Inventaire Forestier, 14 rue Girardet, Nancy 54000, France.
Email: timothee.audinot@laposte.net

Funding information
Laboratory of Excellence ARBRE, Grant/Award Number: ANR-11-LABX-0002-01; Institut national de l'information géographique et forestière

Abstract

Models based on national forest inventory (NFI) data intend to project forests under management and policy scenarios. This study aimed at quantifying the influence of NFI sampling uncertainty on parameters and simulations of the demographic model MARGOT. Parameter variance–covariance structure was estimated from bootstrap sampling of NFI field plots. Parameter variances and distributions were further modeled to serve as a plug-in option to any inventory-based initial condition. Forty-year time series of observed forest growing stock were compared with model simulations to balance model uncertainty and bias. Variance models showed high accuracies. The Gamma distribution best fitted the distributions of transition, mortality and felling rates, while the Gaussian distribution best fitted tree recruitment fluxes. Simulation uncertainty amounted to 12% of the model bias at the country scale. Parameter covariance structure increased simulation uncertainty by 5.5% in this 12%. This uncertainty appraisal allows targeting model bias as a modeling priority.

Recommendations for Resource Managers

- Uncovering the potential and limitations of large-scale forest models are needed when deducing recommendations from forest resource projections under forest management and policy scenarios at regional, national, or continental scales.
- Estimating simulation uncertainty in these models is crucial to assess their accuracy. The present study offers a generic methodological strategy for assessing parameter uncertainty in large-scale forest models.
- Users of the MARGOT model should consider that simulation uncertainties proved to be low at a national scale, but decennial wood stock increases as observed in the French forests over the period 1970–2016 were underestimated.
- Assessing simulation uncertainty is also major for model bias appraisal. Better accounting for the controls of forest demographic processes (growth, regeneration and mortality) appears to be a priority for the development of MARGOT, and for other large-scale models.

KEYWORDS

bootstrap, demographic model, error propagation, forest dynamic, matrix model, national forest inventory, sampling, uncertainty

1 | INTRODUCTION

Forests are essential ecosystems that cover 31% of Earth's terrestrial surface area, are home to the largest share of terrestrial biodiversity (FAO & UNEP, 2020), contribute to terrestrial biogeochemical cycles (Likens, 2013), and sequester carbon (Pan et al., 2011). Forests also play an important role in economy. In 2010, 522 million m^3 of wood were harvested from European forests, including 475 million m^3 of roundwood (Forest Europe, 2015). Their modeling at large scale, in view of quantifying future C stocks and fluxes and wood supply to the forest sector, and their trade-offs, has hence turned essential (Barreiro et al., 2016).

In Europe, forests show an areal expansion resulting from the "forest transition" process (Mather, 1992), mainly due to agricultural land abandonment (Keenleyside et al., 2010). In Europe, forests also demonstrate a rapid increase in volume of the growing stock (Forest Europe, 2015, Bontemps et al., 2020 for France; Egnell et al., 2011 for Sweden; Henttonen et al., 2017 for Finland; and Bontemps, 2021 in Europe). This has arisen from "forest transition"

processes and forest regrowth (Mather, 1992; Rautiainen et al., 2011) and from felling rates being lower than forest growth rates (in 2010, the fellings rates represented 70.5% of the increment of European forests; Forest Europe, 2015), resulting in densification of forests (Bontemps et al., 2020; Rautiainen et al., 2011). Yet, issues of independence from fossil fuels and development of a "green economy" have fostered the bioeconomy strategy initiative (European Commission, 2018), intended to stimulate the use of renewable biological resources (McCormick & Kautto, 2013). In France, the national low-carbon strategy is hence committed to achieving carbon neutrality in 2050 and to increasing the share of renewable energy by 27% in 2030 (Ministry of Ecological Transition, 2020). All these factors make processes of forest dynamics (growth, regeneration, and mortality) and fellings highly nonstationary, and require appropriate models for exploring the integrated consequences of such changes on forests.

For a model to be considered appropriate for projections, an evaluation procedure of different criteria is required (Cariboni et al., 2007; Vanclay & Skovsgaard, 1997), including uncertainty analysis. Model explorations of future forest resources must be able to quantify the uncertainty inherent to the simulation of nonstationary dynamics (Barreiro et al., 2016, 2017) and model reliability. In this study, we use the definition of uncertainty analysis provided by Cariboni et al. (2007) and Tomlin (2013): "uncertainty is the variability of model outputs due to our lack of knowledge in model inputs."

Several large-scale forest dynamic models have been developed in Europe (Barreiro et al., 2016, 2017; Linkevičius et al., 2019) to assist forest strategy development. These models are mainly based on national forest inventories (NFIs; Barreiro et al., 2017) that provide data on the status and trends of forests at regional and national scales (Tomppo et al., 2010). An example is provided by the MELA Finnish simulation platform (Redsven et al., 2013; Siitonen et al., 1996) used to assess the impact of forest management and climate scenarios on future wood availability (Redsven et al., 2013). More recently, the MAtrix model of forest Resource, Growth and dynamics On the Territory scale (MARGOT) model (Wernsdörfer et al., 2012) was used to simulate alternative management and climate scenarios' impacts on the carbon sink of the French forests by 2050 (Roux et al., 2020).

Large-scale models have been evaluated by comparing their simulations to observed NFI-data (e.g., Thürig & Schelhaas, 2006); by sensitivity analysis (e.g., Wernsdörfer et al., 2012); or by measuring parameter uncertainty (Thürig et al., 2005). However, very few large-scale models have undergone full sensitivity analyzes (Barreiro et al., 2016), and in our knowledge, none of them have propagated sampling uncertainty in model simulations of growing stock, associated with model bias assessment related to NFI observations. These uncertainties can originate from the data available to parameterize and initialize the model (sampling methods and errors), from methods of parameter estimation, and from the structure of the model (Van Oijen, 2017). When models are based on survey data such as NFI data, we would expect the sampling error to have a predominant contribution over measurement or model errors (e.g., at least 60% of the total uncertainty for the Catalonia Spanish region according to Fortin et al., 2016).

In this respect, the demographic MARGOT model operating on a partitioning of large forest areas (Wernsdörfer et al., 2012) is worth of investigations, as the French forests to which it is currently applied are highly nonstationary (Bontemps et al., 2020), and the most heterogeneous ones in Europe, covering 13 out of 14 forest types (Barbati et al., 2014). In addition, the French NFI started as early as 1961, providing long-range time series for model evaluation.

The objective of this study was to quantify and model the effect of sampling uncertainty of NFI survey observations on demographic parameters of MARGOT model, to propagate this uncertainty to simulations, and to compare obtained simulations to 40-year time series of

observed forest growing stock at different spatial scales. Since NFI data arise from a statistical sampling process, uncertainty in the initial conditions cannot be distinguished from uncertainty in the whole time series of observations. This larger class of uncertainty was therefore not considered in the assessment of model accuracy.

2 | MATERIAL AND METHODS

2.1 | French NFI data

The French NFI was established in 1958 (Hervé et al., 2014; IGN, 2018). Between 1961 and 2004, the French NFI was based on temporary plots sampled around every 10 years at the "department" administrative unit (*dau*, NUTS-3 unit of the European Community) and asynchronously between *dau*. More clearly, plots in the French NFI are temporary, sampled at *dau* scale and renewed at each inventory occasion. In 2005, NFI sampling of the French forest has turned annual and systematic across space (Bontemps et al., 2020), owing to sampling in a systematic grid every year. Using historical (until 2004) and recent (from 2005 onward) NFI data allows to build long times series of aboveground stem growing stock in metropolitan production forests (sensu forest definition of the FAO, 2005). Data from 1971 onward were used. The first data available from each *dau* spread across a time interval of 14 years (up to 1985) and were used to initialize and parametrize the MARGOT model (Figure S1). Both historical (1971–2004) and recent (2014–2018, aggregated into the median year of 2016 to increase data precision; IGN, 2018) NFI data were used to build annual time series of growing stock by linear interpolation (Figure S1).

Measurements performed on NFI field plots include tree diameter at 1.3 m height and radial increment over 5 years, assumed tree status change over the past 5 years (from living to dead or harvested trees) and tree species (Appendix S1). Of note, between 1961 and 2004, fellings are assumed to having been underestimated by a factor of about 20%–30% at *dau* scale (Bergeot, 2007; Pignard, 1994) and 50%–60% at country scale (Denardou-Tisserand, 2019).

2.2 | Description of the MARGOT model

2.2.1 | Model overview

MARGOT is a deterministic demographic and size-structured matrix model based on Leslie model (Leslie, 1945) and Usher model (Usher, 1966, 1969), whose assumptions are presented in Wernsdörfer et al. (2012). MARGOT is parameterized on a discrete partitioning of French forests across which NFI plots are split, and simulates the tree diameter distribution within each part, also called "stratum." The last diameter class admits no upper limit and is termed "open class." Strata are defined according to fixed forest factors (see Section 2.2.3) and therefore assumed to be independent. The forest demographic processes (transition rate [TR], from one diameter class to another, mortality rate [MR], and felling rate [FR], plus a number of trees growing into the first diameter class as a recruitment flux) are estimated from the samples of trees belonging to one diameter class of a stratum. Forest dynamic processes are assumed to be stationary over time and constant within a stratum. Parameter estimation is described in

Appendix S2. The number of trees per diameter class is converted into growing stock using volume equations of the French NFI.

2.2.2 | Forest partitioning

Partitioning of forests implies to classify each tree of French forest into large homogeneous strata, to both allow aggregating enough trees for inference and accounting for variability of forest dynamics across space (Wernsdörfer et al. 2012). The model parameters (TR, MR, FR, and recruitment) are estimated at the stratum level. Here, a partitioning based on growing stock from recent annual NFI data (2007–2016) to split the number of trees into strata was conducted using the principles from Bontemps et al. (2019) according to (i) forest trees species, (ii) large ecological regions (GRECO) as a biogeographical partitioning of French forests into 11 categories (Cavaignac, 2009; Denardou-Tisserand, 2019; Table S1, Figure S2, and Appendix S2), (iii) ownership categories as subjected to distinct regulation frameworks (private forests, state-owned forests and other public forests owned by municipalities and public institutions). This method means that an NFI plot may be represented in several strata (in the case where more than two species of trees are present on a plot).

The resulting number of strata was reduced by distinguishing individual species when exceeding 1,000,000 m^3 only, the other strata being grouped into generic strata of broadleaves or conifers. The asynchronous sampling of *dau* before 2005 required to define intersections of *dau* and strata, so-called substrata, as simulation units, where too small substrata were discarded. The final partitioning included 135 strata covering 92% of the total growing stock and with more than 1100 NFI plots per stratum on average (SD of >1200 plots/stratum, Table S2), and 700 substrata with more than 200 NFI plots on average (SD of >150 plots/substrata).

2.2.3 | Mathematical formulation

The diameter distribution of the number of trees in a stratum $N_s(t)$ is described in vector form:

$$N_s(t) = \begin{bmatrix} n_{s,1}(t) \\ \vdots \\ n_{s,k}(t) \\ \vdots \\ n_{s,kopen}(t) \end{bmatrix} \quad (1)$$

where $n_{s,k}(t)$ = number of trees in stratum s in diameter class k at time t, where $k = 1, ..., kopen$, and *kopen* denotes the open diameter class.

Over a time-step of the model, a fraction of the number of trees in a diameter class can: (1) remain in the diameter class, (2) move up to the next higher diameter class, (3) die, or (4) be felled. Growth-driven transition rates for the open diameter class do not exist.

Forest dynamic is thus represented in each stratum by two Markov transition matrices that are constant over time. A first transition matrix reflects growth (M_s^+):

$$M_s^+ = \begin{bmatrix} 1 - TR_{s,1\to 2} & 0 & \cdots & \cdots & 0 \\ TR_{s,1\to 2} & \ddots & \ddots & \ddots & \vdots \\ 0 & \ddots & 1 - TR_{s,k\to k+1} & \ddots & \vdots \\ \vdots & \ddots & TR_{s,k\to k+1} & \ddots & 0 \\ 0 & \cdots & 0 & \ddots & 1 \end{bmatrix} \quad (2)$$

where $TR_{s,k\to k+1}$ are the transition rates from a diameter class k to the next diameter class $k+1$, i.e., the proportion of the number of trees moving from a diameter class k to diameter class $k+1$ in a stratum s during one time step. This structure implies than no tree can move two classes or more during one-step time. $TR_{s,k\to k+1}$ estimation is presented in (Equation S1) in Appendix S3.

A second transition matrix (M_s^-) reflects the negative demographic terms (mortality and felling) and is diagonal:

$$M_s^- = \begin{bmatrix} 1 - (MR_{s,1} + FR_{s,1}) & 0 & \cdots & \cdots & 0 \\ 0 & \ddots & \ddots & \ddots & \vdots \\ \vdots & \ddots & 1 - (MR_{s,k} + FR_{s,k}) & \ddots & \vdots \\ \vdots & \ddots & 0 & \ddots & 0 \\ 0 & \cdots & 0 & \ddots & 1 - (MR_{s,kopen} + FR_{s,kopen}) \end{bmatrix} \quad (3)$$

$MR_{s,k}$ is the mortality rate in diameter class k of a stratum s, and $FR_{s,k}$ is the felling rate in diameter class k of a stratum s. $MR_{s,k}$ and $FR_{s,k}$ estimations are presented in Equations S2 and S3 of Appendix S3, respectively.

In each stratum, the recruitment (R_s, presented in Equation S4 in Appendix S3) is the number of trees exceeding 7.5 cm in diameter during a time-step of the model, and reaching the first diameter class only:

$$R_s(t) = R_s = \begin{bmatrix} R_{s,1} \\ 0 \\ \vdots \\ \vdots \\ 0 \end{bmatrix}. \quad (4)$$

The tree diameter distribution, $N_s\ (t+1)$, of a given stratum s at $t+1$ (1-year model time-step as justified below) is predicted by the following equation based on the one at time t, $N_s\ (t)$:

$$N_s(t+1) = M_s^- \times \left(R_s + M_s^+ \times N_s(t)\right). \quad (5)$$

This model formulation is a revision of the basic one presented in Wernsdörfer et al. (2012), to better account for the sequence of the different demographic processes (growth, recruitment, mortality, and felling) as reflected in the NFI data.

Once the demographic projections have been carried out, the numbers of simulated trees are converted into volume (in m^3):

$$v_{s,k}(t) = N_{s,k}(t) \times \bar{v_{s,k}}, \quad (6)$$

where $v_s(t)$ gives the total volume per diameter class in stratum s and in diameter class k at time t, and $\bar{v}_s$ the mean individual stem volume per diameter class in stratum s and in diameter class k (volume equation), assumed to be constant over time.

Standing volume (in m^3) predicted by the model is provided by the following equation at national scale:

$$v_{ff}(t) = \sum_{s,k} v_{s,k}(t), \tag{7}$$

where $v_{ff}(t)$ gives the total volume in French forest (ff) at time t.

2.2.4 | Model time step and width of diameter classes

In general, the number and width of diameter classes result from tradeoffs between the model time step, the sampling error and the difference between discrete distribution of individual population in the matrix model and its continuous counterpart (Picard et al., 2010). In this study, the width of the diameter classes was set to 10 cm. The highest diameter class was defined as an open class (i.e., without upper limit) for each stratum (Appendix S4 and Table S2). Inventory data used for model initialization and parameterization are presented in Table S3.

The model is designed for discrete-time used. The historical NFI data structure (asynchronous sampling) imposed an annual time step over the simulation period for synchronization of simulations across strata.

2.3 | Assessing model parameter uncertainty by bootstrap resampling

While inference of demographic rates (ratios of the number of trees), including their averages and errors, can theoretically be derived as design-based estimators in a statistical NFI, this approach has not been derived and made available to date, in a context where the estimation of absolute demographic fluxes in forests have been changed very recently and rely on successive samples. Therefore, an empirical bootstrap resampling approach could not be avoided in this study, for the present purpose of estimating errors of the demographic rates.

The leading principle of the present approach was to infer uncertainty in model parameters, namely their standard deviations (SD), distributions, and covariance, by implementing a bootstrap method with replacement.

In the NFI survey, NFI plots of a stratum, not trees, form the primary sampling units (Figure 1). The resampling process was therefore performed at this scale and assumes that the NFI plots were sampled with replacement with equal probability in the French forests (Gregoire & Valentine, 2007).

To assess the appropriate number of bootstrap samples requested for each sampling rate, three reference strata were selected, including two strata of extreme initial size (21 and 9113 plots, termed Minstratum and Maxstratum, respectively), and one random additional one (121 plots, termed Ranstratum, see Appendix S5). In each reference stratum, a standard range of seven bootstrap sample sizes was explored (100, 250, 500, 1000, 2500, 5000, and 10,000).

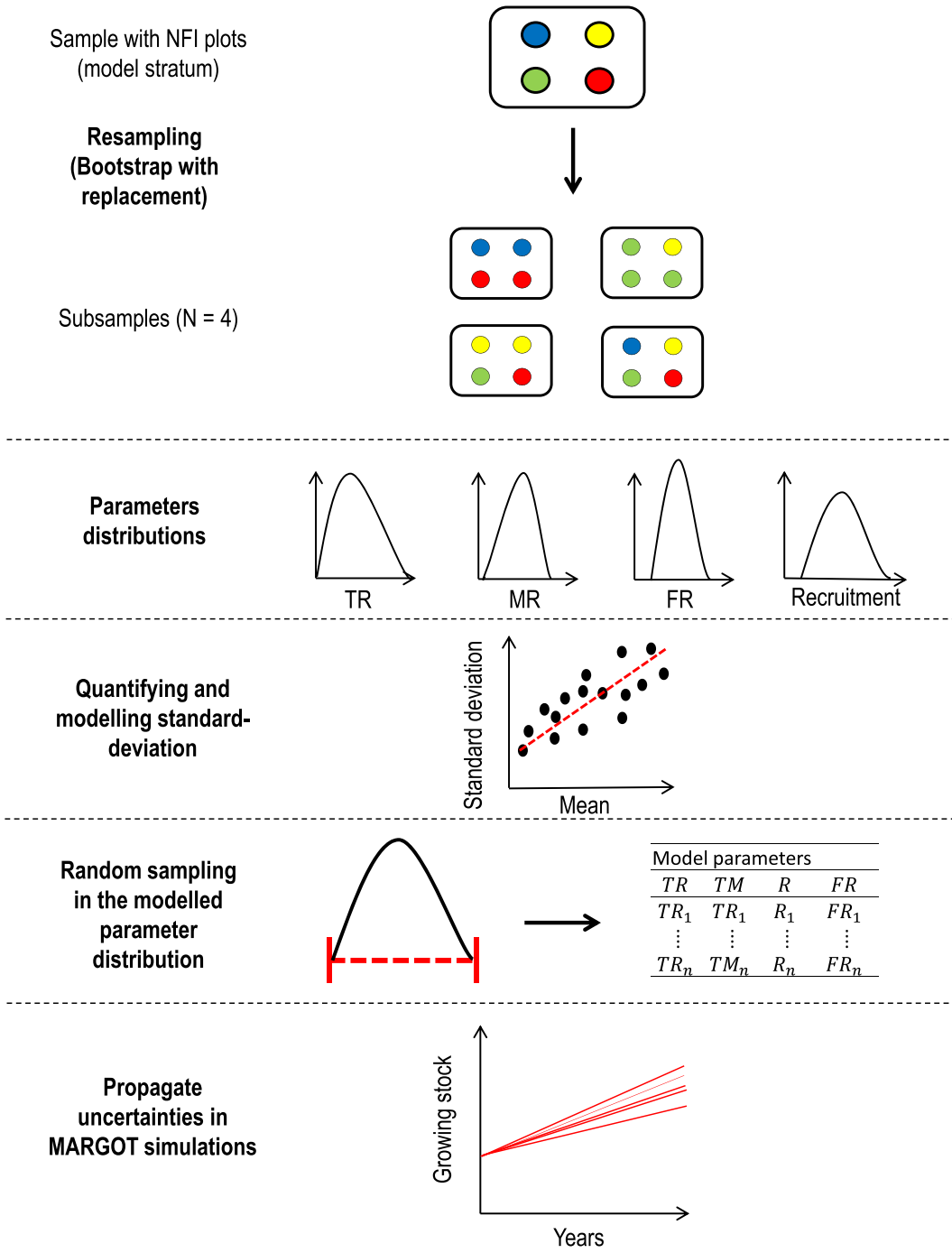

FIGURE 1 Flowchart of methods used to quantify the sampling uncertainty of NFI observations on the parameters and propagate it in the simulations of MARGOT. FR, felling rate; MR, mortality rate; R, Recruitment; TR, transition rate.

To determine bootstrap sample size, the coefficient of variation (CV) of bootstrap parameter distributions was computed (called CV_{sample}):

$$CV_{sample} = \frac{\sigma_{sample}}{\mu_{sample}} \times 100, \quad (8)$$

where σ_{sample} was the standard deviation and μ_{sample} was the mean of the bootstrap parameter distributions.

2.4 | Parameter distribution inference and modeling

Bootstrap parameter distributions would have been in principle sufficient to evaluate simulation uncertainty. Nevertheless, a further goal was to develop a plug-in parameter uncertainty model on initial NFI cycles that may be different from the ones used in this contribution for the sake of flexibility (for instance, the last NFI cycle for exploring forest projection in the future). Models for parameter distribution and SD were therefore needed.

2.4.1 | Probability laws of parameter distributions

By their nature, the parameters TR, FR, and MR take their value in the [0;1] interval whereas the recruitment parameter is only subjected to be positive. However, distributions that take their values outside these ranges are conceivable as soon as their parameter values ensure that the probability of taking a value outside is negligible. That is why we have tested distributions such as the Gaussian one that can take any real value.

A Kolmogorov–Smirnov test (Birnbaum & Tingey, 1951) was performed on parameter distributions to determine which of the following reference distributions best fitted the data across the standard range of sampling rate:

- The Gaussian distribution ($X \sim N(\mu, \sigma^2)$) as a reference distribution for average rates and recruitment parameters.
- The log-normal distribution (where the natural logarithm of the variable is $N(\mu, \sigma^2)$) as an alternative allowing to account for a right asymmetry.
- The continuous uniform distribution ($X \sim U(a, b)$) as a reference distribution between maximum and minimum in parameter distributions.
- The two-parameter Beta distribution ($X \sim \text{Beta}(\alpha, \beta)$), defined on [0, 1] like demographic rates, allowing to account for a right asymmetry in parameters.
- The two-parameter Gamma distribution ($X \sim \text{Gamma}(k, \theta)$) that both allows a right asymmetry in parameter distributions and flexibility on the left-side of the distribution (possible inflection point).

The percentages of appropriate fits to each of these distributions at each sampling rate were computed and analysed at p values thresholds of .05 and .01.

2.4.2 | Modeling of parameter SDs

Bootstrap SD were computed for all parameters in all strata. To be able to predict them for future average parameter sets (e.g., at another historical period), these errors were modeled by linear regression against parameter means, tree diameter classes, and strata. Modeled distributions (based on reference distribution choice and sampling errors) were compared against empirical bootstrap distributions. Three nested linear regression models were tested.

In a first base model, parameter SD were regressed against parameter averages. To control for the heteroscedasticity observed in this relationship, models were fitted on a logarithmic scale:

$$\text{Model } 1 \rightarrow \log(\sigma) = a + b \times \log(\mu) + \varepsilon, \tag{9}$$

where σ and μ were the SDs and parameters averages, respectively, a and b were the model coefficients and $\varepsilon \sim N(0, \sigma^2)$.

A residual structure found with diameter class (k, treated as a factor) yielded a second model to be tested:

$$\text{Model } 2 \rightarrow \log(\sigma_k) = a_k + b \times \log(\mu_k) + \varepsilon. \tag{10}$$

Finally, a third model was tested with strata (s, treated as a factor):

$$\text{Model } 3 \rightarrow \log(\sigma_{k,s}) = a_{k,s} + b \times \log(\mu_{k,s}) + \varepsilon. \tag{11}$$

Recruitment being estimated only for the first diameter class in each stratum. Therefore, only the Model 1 was applied to the recruitment distributions.

2.4.3 | Variance–covariance matrix of parameters

Variance–covariance matrices of parameter sets were estimated from bootstrap parameters distributions at stratum scale. Variances of model parameters were provided by SD models (see Section 2.4.2). In view of the unrealistic effort of covariances' modeling (maximum 351 models per stratum), we used correlation estimates as directly inferred from the bootstrap samples.

The variance–covariance matrix is used to replicate multiple random samples of model parameters from a Gamma distribution (see below). For this, the multidimensional rmvgamma function of the lcmix package (Dvorkin, 2012) in R generates a random sample from the correlation matrix. As an exploratory approach, 1000 parameter sets were resampled.

2.5 | Propagation of parameter uncertainty in MARGOT simulations

Simulations were performed at a substratum scale (stratum split by *dau*) and were analyzed from the date when data from all the *dau* of a stratum were available.

At stratum scale, 1000 simulations were performed (i.e., a total of 135,000 simulations) from the 1000 sets of parameters randomly assembled. These simulations were then

summed up to obtain 1000 simulations of forests at the country scale. This allowed assessing variability in total growing stock at the end year of simulation (2016), at both strata and country scales.

To assess the influence of the covariance structure in simulations, the approach was repeated with/without a/any variance–covariance matrices, where either a diagonal structure or the empirically estimated correlation matrix were compared.

In view of stratum size variability (mean of 11,000,000 m^3 and SD of 14,000,000 m^3, Table S2), *CV* (called $CV_{uncertainty}$) of final growing stocks were computed to compare the propagation of parameter uncertainty across strata at the end of simulations:

$$CV_{uncertainty} = \frac{\sigma_{simulation}}{\mu_{simulation}} \times 100, \tag{12}$$

where $\sigma_{simulation}$ was the standard deviation and $\mu_{simulation}$ was the mean of the 1000 simulations performed at stratum or country scales.

Moreover, strata were gathered into four quartiles with respect to their initial size (number of NFI plots), and into three groups with respect to their initial parameter number, depending on the number of diameter classes; modest, mid, and large groups (Table 1). This allowed exploring dependence on these factors.

To compare the model bias to the relative dispersion of the simulations (measured by $CV_{uncertainty}$, a *CV* (called CV_{bias}) was computed as follows at stratum and country scales:

$$CV_{bias} = \frac{bias_{simulation}}{\mu_{simulation}} \times 100, \tag{13}$$

where $bias_{simulation}$ was the model bias.

TABLE 1 Description of quartiles of strata distributed according to their number of national forest inventory plots and of groups of strata distributed according to their number of diameter classes

		Mean number of NFI plots	SD of the number of NFI plots	Mean number of diameter classes	SD of the number of diameter classes	Number of strata
Inventory plot quartiles	1	266	121	5.4	1.4	34
	2	572	83	5.7	1.1	33
	3	967	173	6.3	1.2	34
	4	2 663	1 673	6.7	1.5	34
Diameter class groups	Modest group	709	896	3.9	0.2	22
	Norm group	805	541	5.6	0.5	65
	Large group	1 738	1 765	7.6	0.7	48

Note: Modest group: strata having 3–5 diameter classes. Norm group: strata having 6–7 diameter classes. Large group: strata having more than 7 diameter classes.

Abbreviation: NFI, national forest inventory.

3 | RESULTS

3.1 | Analysis of bootstrap parameter distributions

The stability analysis of bootstrap parameter distributions led us to fix bootstrap sample size at 1000 units (Section 2.3 and Figure S3). Means and SD of demographic rates were found more variable in the high diameter classes (Figures S4 and S5). The number of inventory plots being lower in high diameter classes compared to the others, this result appeared logical.

However, means and interquartile of MR were found also variable across the first diameter classes (Figures S4b and S5b). Tree mortality was rarer, but it affected young trees (e.g., competition) and old trees (e.g., disease) more than other trees, yielding a logical U-shaped distribution of the parameter across diameter classes. On the other hand, means and SD of fellings rate increased with the diameter classes (Figures S4c and S5c), as a larger share of large trees than of small trees is usually harvested.

The grand mean of recruitment distributions was 1,215,000 trees, while the average SD of recruitment distributions was 170,000 trees.

3.2 | Probability laws for parameter distributions

Kolmogorov–Smirnov tests showed that demographic rates parameters distributions (TR, MR, and FR) much more frequently fitted a Gamma distribution than any other one (Table 2).

Gamma distributions more frequently fitted demographic rates than Beta distributions (Table 2), while log-normal distributions were less frequently fitted than Gaussian distributions across all parameters (Table 2). Parameter distributions of demographic rates never fitted a uniform distribution (Table 2).

The proportion of distributions of FR fitting a Gamma distribution was greater than for the other parameters (Table 2). These distributions were therefore more often asymmetric.

In view of these results, for demographic rates parameters, a Gamma distribution was adopted as a reference probability model for simulations.

The largest share of distributions fitting the Gaussian distribution was found for recruitment (Table 2). However, the share of recruitment distributions following a Gamma distribution was very close. Therefore, the Gamma distribution was retained for recruitment as a reference probability model for simulations like for demographic rates.

3.3 | Modeling of parameter SDs

Model 3 (Equation 11) showed high R^2 (.94 for both TR and FR and .96 for MR, Table 3) and performed significantly better than Model 1 and Model 2 (respectively Equations 9 and 10, $p < 10^{-10}$ in both cases, Table 3). However, Model 2 showed also high R^2 (respectively .78, .80, and .86 for TR, FR, and MR, Table 3). In addition, Model 2 allowed correcting for the initial bias found along the diameter classes and performed significantly better than Model 1 ($p < 10^{-10}$, Table 3). Therefore, to use an efficient and sparse model, Model 2 was retained on the original initial conditions of the study. Accuracy of Model 2 with the different predictors is presented in Figures S9, S10, and S11.

TABLE 2 Percentage of MARGOT parameters' distributions fitting to the Gaussian, log-normal, uniform, Beta, and Gamma distributions

Probability law	Parameter of MARGOT	Share of parameter distributions fitting reference distributions (%)	
		$p < .05$	$p < .01$
Gaussian distribution	TR	59.5	72.9
	FR	58.4	73.6
	MR	33.0	46.0
	Recruitment	80.7	88.9
Log-normal distribution	TR	40.8	54.5
	FR	61	74.0
	MR	29.6	37.9
	Recruitment	60.0	74.1
Continuous uniform distribution	TR	0	0
	FR	0	0
	MR	0	0
	Recruitment	3.0	3.7
Beta distribution	TR	8.9	19.2
	FR	26.0	40.4
	MR	46.4	54.1
	Recruitment	0	0
Gamma distribution	TR	69.7	75.6
	FR	85.9	89.7
	MR	52.3	57.7
	Recruitment	79.3	84.4

Abbreviations: FR, felling rate; MR, mortality rate; TR, transition rate.

For recruitment, Equation (9) showed high R^2 (.96, Table 3) and was not biased (Figure S13). Accuracy from is presented in Figure S12.

3.4 | Variance–covariance matrix

The variance–covariance matrices were estimated across parameters of each stratum (Section 2.4.3). The covariance structure was found to be weak for all strata. The strongest correlations were positive and found between the same demographic rates of adjacent diameter classes. Weak negative correlations were logically correlation matrices in Figure S13 illustrate these findings on the three reference strata (Maxstratum, Minstratum, and Ranstratum).

TABLE 3 Performance of standard-deviation models of demographic parameters

Parameter of MARGOT	Model	R^2	RSS	*p* value (*F* test)	AIC
TR	Model 1	.65	199	–	1089
	Model 2	.78	126	$<10^{-10}$	801
	Model 3	.94	36	$<10^{-10}$	237
FR	Model 1	.70	214	–	1217
	Model 2	.80	146	$<10^{-10}$	928
	Model 3	.94	44	$<10^{-10}$	251
MR	Model 1	.72	203	–	1051
	Model 2	.86	102	$<10^{-10}$	661
	Model 3	.96	32	$<10^{-10}$	251
Recruitment	Model 1	.96	125	–	−64

Note: *p* Value = significance of model comparisons from ANOVA test.

Abbreviations: AIC, Akaike information criterion; RSS, residual sum of squares.

3.5 | Propagation of parameter uncertainty into model simulations

3.5.1 | Propagation of parameter uncertainty at country and strata scale

Simulations at the country scale (Figure 2), and for the three reference strata (Maxstratum, Ranstratum, and Minstratum, Figure 3) showed a linear increase of simulation uncertainty over the simulation period, in line with the multiplicative structure of the model.

The growing stock increased by +27.7 million m^3/year over the 1985–2016 period at the country scale (period in which NFI data was available for all strata). MARGOT simulated an increase between +16.3 and +20.4 million m^3/year over the same period at the country scale (corresponding to upper and lower quantiles respectively, in simulations with covariance structure at the country scale (Figure 2a). MARGOT was able to replicate the growing stock trend across the country but severely underestimated it.

Simulation uncertainties (represented by $CV_{uncertainty}$, Section 2.5) at the country scale in 2016 were 1.8/1.7% with/without covariance structure and SD were 40/37 millions m^3, while model biases were −332 million m^3 (NFI observation compared to the mean of simulations, Figure 2), that is, CV_{bias} was 14.8% with covariance structure. Therefore, simulation uncertainty at country scale over a 40-year simulation period correspond only to 12% of the final model bias (with covariance structure).

$CV_{uncertainty}$ of strata in 2016 were 10.9/10.3% with/without covariance structure and means of SD were 1.8/1.7 million m^3 (Figure 4), while means of model biases were −2.5 million m^3 with and without covariance structure (with a SD of 13.5 million m^3; NFI observations compared to the means of simulations at stratum scale). At stratum scale, simulation uncertainty was much closer to simulation bias, but remained lower.

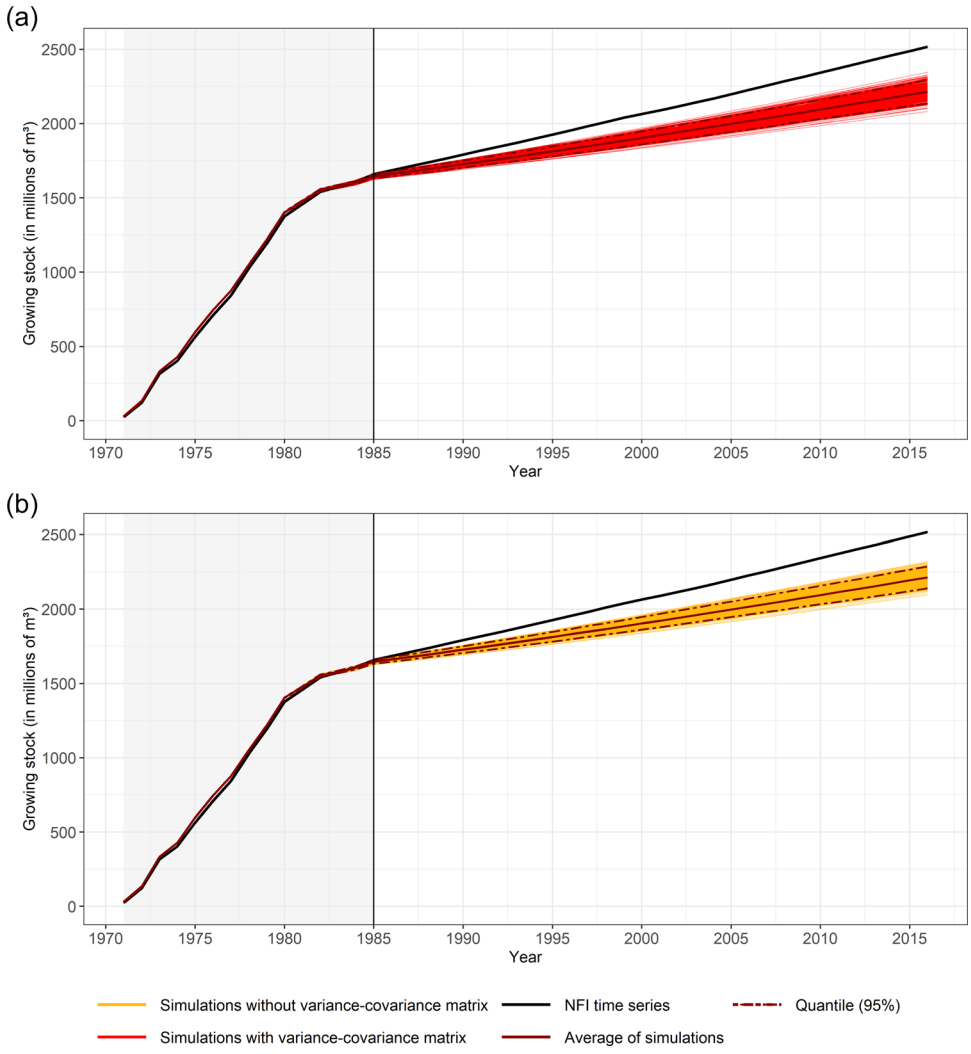

FIGURE 2 Propagation of parameter uncertainty in MARGOT simulations at country scale over a 40-year simulation period with (a)/without any (b) covariance structure. The shaded rectangle corresponds to years for which NFI data for the whole of the French forest are not available. Vertical black line indicates from which year onward inventory data is available for the whole of the French forest.

3.5.2 | Variance–covariance matrix influence on simulation uncertainty

Despite the weakness of individual correlations between model parameters of a stratum (Section 3.4), inclusion of covariance structure in the propagation of parameter uncertainty significantly increased the simulation uncertainty ($p < .05$, Figure 5), in logical accordance with the negative correlations between TR/MR and TR/FR parameters reflecting opposed demographic effects, and therefore amplify the intrinsic parameter uncertainty.

Simulation uncertainty was also significantly less important in strata of greater initial size ($p < .01$ as observed both with and without any covariance structure between the first and fourth quartiles, Figure 5a). Moreover, taking the covariance matrix into account mostly

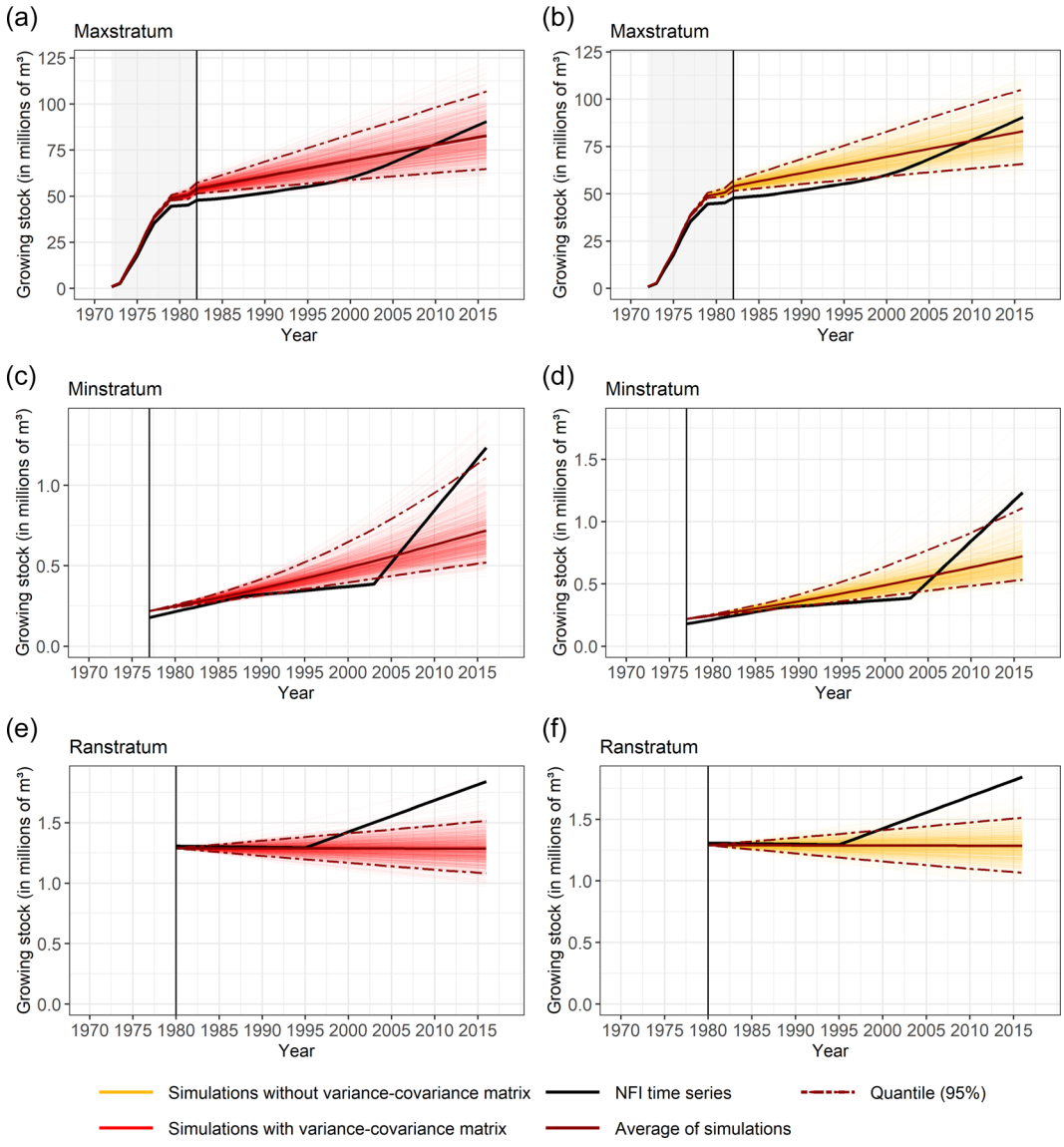

FIGURE 3 Propagation of parameter uncertainty in MARGOT simulations at strata scale with/without any covariance structure. The shaded rectangle corresponds to years for which NFI data for the whole of the French forest are not available. Vertical black line indicates from which year onward inventory data is available for the whole stratum. Maxstratum: various broadleaves in private forests of central France. Minstratum: various conifers in private forests of Corsica. Ranstratum: various broadleaves in state-owned forests of Brittany.

impacted small strata ($p < .01$ both first and second quartiles, respectively, Figure 5a). Since strata of extreme size were considered here, an outcome is therefore that the magnitude of uncertainty in simulations is directly influenced by the range of stratum size, the latter depending on how forest partitioning was defined and how many plots the NFI can provide. This also gives a posterior rationale for the aggregation of small strata into broader generic ones (Section 2.2.2 and Appendix S2).

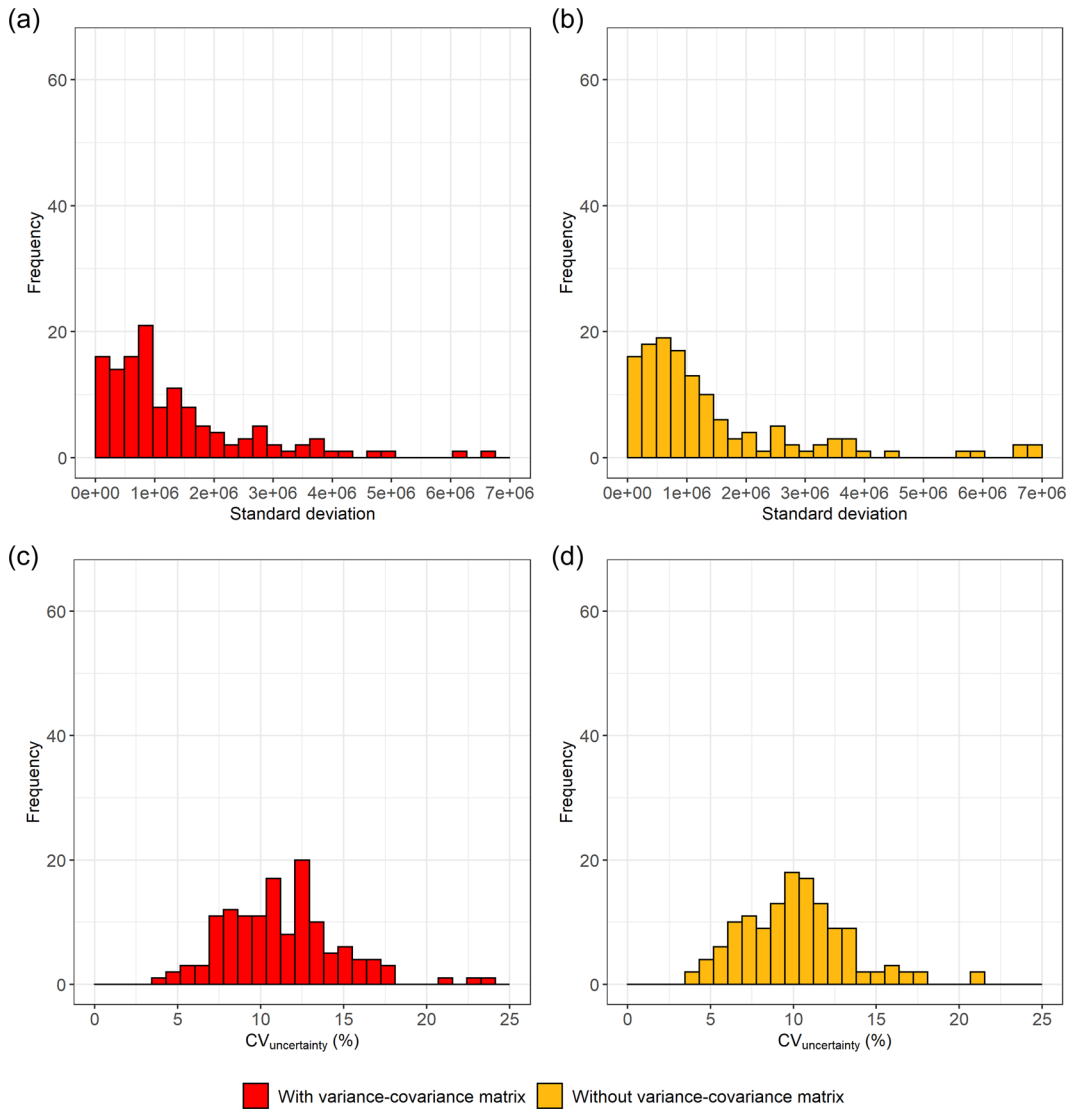

FIGURE 4 Distributions of SDs (a, b) and coefficients of variation (CV; c, d) measuring the propagation of parameters uncertainty in MARGOT simulations at strata scale with/without any covariance structure.

3.5.3 | Diameter class number effect

Simulation uncertainty did not differ significantly between diameter class groups (Figure 5b). These results indicated that the number of parameters did not influence the simulation uncertainty. Moreover, strata with >7 diameter classes also corresponded to a high mean number of NFI plots (1738, Table 1), able to decrease simulation uncertainty (Figure 5a). Therefore, the influences of parameter number and stratum size on simulation uncertainty could not be clearly separated.

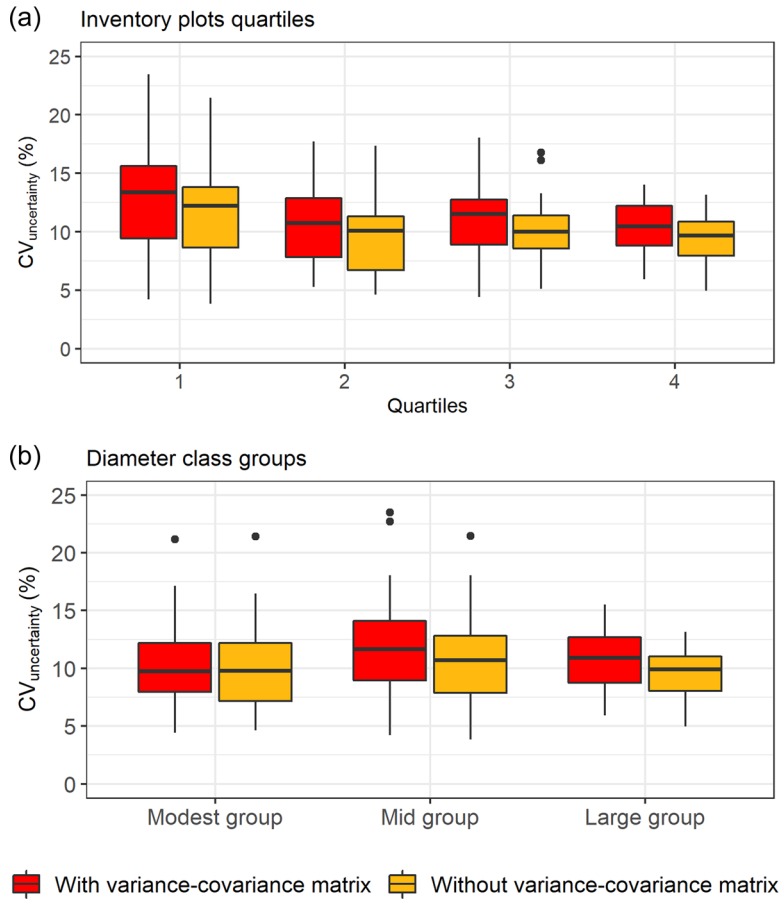

FIGURE 5 Assessment of dispersion (CV) of MARGOT projections according to the number of national forest inventory plots (a) and the number of diameter classes (b) in a stratum, with/without any covariance structure. Black points are outliers. Modest group: strata having 3–5 diameter classes. Norm group: strata having 6–7 diameter classes. Large group: strata having more than 7 diameter classes.

4 | DISCUSSION

4.1 | Sources of uncertainty

In this study, a bootstrap resampling of NFI plots used to initialize and parameterize MARGOT model was implemented, to quantify the uncertainty in tree demographic parameters (TR, MR, FR, and recruitment) stemming from NFI survey sampling and model their distributions. Parameter uncertainty was then propagated in MARGOT simulations at stratum and country scales to quantify simulation uncertainty and balance it with model bias.

Uncertainties on the initial conditions of the model, namely initial tree populations in diameter classes, have not been considered in this study. This uncertainty indeed applies at each inventory occasion that produces longitudinal data for model validation and raises the more general question of model evaluation on uncertain data. The uncertainty of the number of trees may also be obtained from the bootstrap samples, or from standard estimators for

stratified sampling (Mandallaz, 2008). This method was notably used by Fortin et al. (2016) on the Spanish national forest inventory.

Other sources of uncertainty for initial conditions and parameters concern measurement errors and observer variability (McRoberts & Westfall, 2014). These uncertainties have been the subject of several studies (e.g., Berger et al., 2014; McRoberts & Lessard, 2001; Westfall & Patterson, 2007). We are not aware of any attempt at propagating such uncertainty in regional and country-oriented forest modeling.

4.2 | Initialization and parameterization of MARGOT

The size of the strata on which MARGOT operated was very variable (with a SD of 14,000,000 m^3 for a mean of 11,000,000 m^3, Table S2), so was the number of NFI plots in each stratum (SD of 1253 NFI plots for a mean of 1121 NFI plots, Table S2). Simulation uncertainty was found larger with a lower number of NFI plots in a stratum (Figure 5a), which showed the influence of the number of NFI plots on parameter uncertainty. There was therefore a trade-off between the number of forest strata reflecting driving factors of forest dynamics (Wernsdörfer et al., 2012) and simulation precision related to parameter uncertainty (a higher number of NFI plots per stratum implied a lower number of strata). Therefore, we argue that during the stage of partitioning a forest resource for a large-scale forest model, it is necessary both to create strata representative of diversity of forest resource under study and of sufficient sizes to limit propagation uncertainty in model simulations. This may form a matter of further research.

Diameter class width was set at 10 cm, close to the value determined by Picard et al. (2010) on tropical trees (11.4 cm). This diameter class width in Picard et al. (2010) was based on a trade-off between sampling error and the difference between discrete distribution of individual populations in the matrix model and its continuous counterpart. In other words, smaller diameter classes reduce bias in parameters but increase uncertainty due to a smaller sample size per class. However, a low width of diameter classes allows for increasing the tree proportion that passes from one class to another one, among the total number of trees in a stratum. We, therefore, hypothesize that smaller diameter classes would increase forest dynamic in MARGOT simulations and reduce the underestimation (−332 million m^3) of the NFI data time series. It is therefore a priority to test whether the trade-off between uncertainty and bias would be more balanced when diameter class width was reduced.

4.3 | Bootstrap initialization

Bootstrap was performed with 1000 subsamples of each parameter in a stratum. However, for the three strata used, the convergence threshold of CV_{sample} (see Section 2.3) was between 1000 and 2500 subsamples, and rather at 2500 subsamples for few sampling rates (Figure S3). Thus, it would be more cautious to estimate the parameter distributions from 2500 subsamples. CV_{sample} in Maxstratum (comprising 9113 NFI plots) further converged faster than those in Ranstratum and Minstratum (comprising, respectively, 120 and 21 NFI plots), suggesting that bootstrap sample number should be optimized at stratum level in future developments.

4.4 | Approximated probability laws for parameter distributions

A Gamma law frequently fitted demographic rate distributions (Table 2), with a right skewness often observed (Figures S6, S7, and S8). However, symmetry did not have the same magnitude for the different demographic rates and was found strongest for the MR (on average 1.07 with an SD of 0.59). The rarity of mortality events may explain this result. However, asymmetry (measured by the skewness coefficient) was weaker for FR (on average 0.66 with an SD of 0.40) which also forms a rare event in the forests (on average 12.0% of NFI plots within a stratum and a diameter class contain at least one felled tree, with an SD of 7.9%). While demographic rates are estimated from the number of trees, NFI plots, not trees, were the sampling units of the study, with a possible impact on the distribution of demographic rates of an over-represented event in one or a few NFI plots.

Gaussian law also fitted with a large fraction of parameter distributions (Table 2), especially those where the asymmetry was low, as in the case of recruitment (mean asymmetry of 0.55 with an SD of 0.33). However, the Gamma law yielded comparable outcomes (Table 2) and remains technically more practical, as it is set to values strictly >0, and avoids the situation of negative rates. Beta and log-normal distributions were also tested but were less accurate than the Gamma and Gaussian distributions (Table 2). In addition, a little fraction of recruitment distributions fitted a uniform law (3%, Table 2).

4.5 | Parameter distributions and measurement of uncertainties

The variance–covariance matrices were estimated from bootstrap parameter distributions. Covariances between parameters were not modeled, unlike the SD, as it appeared out of practical reach (maximum 351 models per stratum).

Correlations between parameters were found generally small. Yet, correlations between forest dynamic processes are well established, including a negative correlation between growth and mortality (Zhu et al., 2017), and a positive correlation between growth and fellings. Accordingly, we observed some negative correlations between TR and MR, but also between TR and FR (Figure S13). The latter negative correlations can find root in that, with more trees harvested, the number of trees that can potentially transit from one diameter class to another decrease. As an explanation for the weakness of parameter correlations, stratum-based partitioning of vast forest territories represents forest ensembles by far larger than usual management units in homogeneous forests (usually several tens of hectares), making correlations between demographic parameters much less discernible beyond a certain spatial scale. Analyzing the relationships between stratum size and parameter correlation strength would provide the first demonstrative indications in this respect.

The very high accuracy of models for parameter standard deviations (Table 3) for accessing to parameter uncertainty make them useable on any inventory-based initial condition, and in the case where these parameters would be dynamic (e.g., scenario-driven) over a simulation period. These models thus make it possible not to perform the bootstrap random resampling step on NFI databases each time the model is used, and substantially increase the practical handling and quantification of simulation uncertainty. This generic methodology for assessing parameter and simulation uncertainties can be applied to all forest models based on NFI data.

4.6 | Propagation of parameter uncertainty in model simulations

One thousand parameter sets were sampled from the Gaussian distributions to measure simulation dispersion. However, there were $C41{,}000 = 4.14 \times 1010$ possible theoretical combinations of the four parameter sets, based on 1000 bootstrap samples per parameter. It is therefore likely that, with only 1000 simulations, the propagation of parameter uncertainty was greatly underestimated. A Series of simulations having different reasonable numbers of simulations (e.g., 1000, 2500, 5000, and 10,000) could be performed to measure the influence of a number of simulations on uncertainty propagation.

Despite the weak correlations between model parameters, including the parameter covariance structure in their simulations increased the simulation uncertainty by +5.5% at stratum and country scales when comparing $CV_{uncertainty}$ of the simulations ($p < 0.05$ at both scales, Figures 2–5). Therefore, a larger number of parameters in a large-scale model will generate greater uncertainty, and this stresses the need for compact models of forest dynamic. In addition, we agree with the conclusions of Breidenbach et al. (2014) who recommended the systematic use of the covariance structure of forest model parameters to measure their uncertainties.

Also, the model was able to simulate the increase in forest growing stock (Bontemps et al., 2020) at country scale over the 1985–2016 period (Figure 2). This tendency of expansion was already simulated by MARGOT in the study by Wernsdörfer et al. (2012) and by the EFDM matrix model (Vauhkonen et al., 2019), for a future period in both cases. Our study dealing with a past period monitored by NFI data allowed to detect that the expansion simulated by MARGOT was underestimated (by 332 million m^3 over the study period). In addition, the increasing trend in growing stock at country scale over the 1985–2016 period observed in the NFI data (+27.7 million m^3/year) was not included in the simulation range of MARGOT (between +16.3 and +20.4 million m^3/year), pointing out to a substantial model bias in this respect.

MARGOT model so far assumes that demographic parameters are constant over time (Wernsdörfer et al., 2012) and across a stratum. However, the growing conditions and hence dynamics of most forests have been changing over recent decades, with changes differing between tree species and regions (Charru et al., 2017; Ols et al., 2020). Consequently, considering this nonstationarity of forests in the model is a matter of ongoing model development. Using the model with nonconstant parameters also stresses the need to predict uncertainty in the parameters at each time step where they would change during a model simulation.

Last, fellings in historical NFI data have been shown to be underestimated by about 50%–60% at country scale (Denardou-Tisserand, 2019), which increases the bias observed in Figures 2 and 3. Simulation uncertainty corresponded only to 12% of the model bias at the country scale (see Section 3.5.1). Therefore, although measurement of uncertainties has been identified as a necessity for large-scale models (Barreiro et al., 2017), increasing the accuracy of such large scale-models by accounting for environmental (climate) and demographic (density) factors that make parameters variable in time also forms a priority for these models (Vauhkonen & Packalen, 2018).

5 | CONCLUSIONS

- Resampling of inventory plots that are at the basis of the MARGOT model allowed estimating the distributions of model demographic parameters (TR, MR, FR, and tree recruitment fluxes). These distributions more frequently fitted a Gamma distribution than other candidate distributions.

- Parameter uncertainty (SD) was modeled as a function of parameter mean and diameter class with high goodness of fit, providing a tangible basis for parameter uncertainty propagation in contexts where parameters will change over time.
- The method implemented here can be applied to any field-sampling data-based forest dynamics model.
- Simulation uncertainty decreased with an increasing number of sampling units within a forest stratum, stressing the need for aggregation of sampling units into a limited number of homogeneous strata.
- Parameter covariance structure was found to significantly increase simulation uncertainty, in accordance with well-known correlations of forest dynamic processes.
- Simulation uncertainty over 40 years was low compared to model bias at country scale. However, uncertainty can be very high at stratum level and must therefore be systematically evaluated at all scales.
- Bias reduction forms a priority to be addressed in model development and may be reached when the nonstationary context of forest dynamics will be better considered.

AUTHOR CONTRIBUTIONS

Timothée Audinot: Conceptualization (equal); data curation (equal); formal analysis (equal); investigation (equal); methodology (equal); writing–original draft (equal). **Holger Wernsdörfer**: Conceptualization (equal); data curation (equal); formal analysis (equal); funding acquisition (equal); investigation (equal); methodology (equal); project administration (equal); supervision (equal); writing–original draft (equal). **Gilles Le Moguédec**: Formal analysis (equal); methodology (equal); validation (equal). **Jean-Daniel Bontemps**: Conceptualization (equal); data curation (equal); formal analysis (equal); funding acquisition (equal); investigation (equal); project administration (equal); methodology (equal); supervision (equal); validation (equal); writing–original draft (equal).

ACKNOWLEDGMENTS

We are particularly grateful to Guillaume Chauvet (ENSAI) and Olivier Bouriaud (Stefan cel Mare University of Suceava) for their contribution to methodology and reviewing. This study was part of the PhD project of T. Audinot funded by the French institute of geographic and forest information (Institut National de l'Information Géographique et Forestière, IGN). The Laboratory of Forest Inventory and UMR SILVA are supported by a grant overseen by the French National Research Agency (ANR) as part of the « Investissements d'Avenir » program (ANR-11-LABX-0002-01, Lab of Excellence ARBRE).

CONFLICT OF INTEREST

The authors declare no conflict of interest.

DATA AVAILABILITY STATEMENT

The data that support the findings of this study are available on request from the corresponding author. The data are not publicly available due to privacy or ethical restrictions.

ORCID

Timothée Audinot http://orcid.org/0000-0001-9716-7170
Gilles Le Moguédec https://orcid.org/0000-0002-7292-9121

REFERENCES

Barbati, A., Marchetti, M., Chirici, G., & Corona, P. (2014). European forest types and forest Europe SFM indicators: Tools for monitoring progress on forest biodiversity conservation. *Forest Ecology and Management*, *321*, 145–157.

Barreiro, S., Schelhaas, M. J., Kändler, G., Antón-Fernández, C., Colin, A., Bontemps, J. D., Alberdi, I., Condés, S., Dumitru, M., Ferezliev, A., & Fischer, C. (2016). Overview of methods and tools for evaluating future woody biomass availability in European countries. *Annals of Forest Science*, *73*(4), 823–837.

Barreiro, S., Schelhaas, M. J., McRoberts, R. E., & Kändler, G. (Eds.). (2017). *Forest inventory-based projection systems for Wood and Biomass Availability* (Vol. 29). Springer.

Bergeot, F. (2007). *Estimation du prélèvement en forêt par l'Inventaire forestier national—Historique. Document interne*. IFN.

Berger, A., Gschwantner, T., McRoberts, R. E., & Schadauer, K. (2014). Effects of measurement errors on individual tree stem volume estimates for the Austrian National Forest Inventory. *Forest Science*, *60*(1), 14–24.

Birnbaum, Z. W., & Tingey, F. H. (1951). One-sided confidence contours for probability distribution functions. *Annals of Mathematical Statistics*, *22*(4), 592–596.

Bontemps, J. D. (2021). Inflation of wood resources in European forests: The footprints of a big-bang. *PLoS One*, *16*(11), e0259795.

Bontemps, J. D., Denardou, A., Hervé, J. C., Bir, J., & Dupouey, J. L. (2020). Unprecedented pluri-decennial increase in the growing stock of French forests is persistent and dominated by private broadleaved forests. *Annals of Forest Science*, *77*(4), 1–20.

Bontemps, J. D., Hervé, J. C., & Denardou, A. (2019). Partition idéalisée et régionalisée de la composition en espèces ligneuses des forêts françaises. *Écoscience*, *26*(4), 291–308.

Breidenbach, J., Antón-Fernández, C., Petersson, H., McRoberts, R. E., & Astrup, R. (2014). Quantifying the model-related variability of biomass stock and change estimates in the Norwegian National Forest Inventory. *Forest Science*, *60*(1), 25–33.

Cariboni, J., Gatelli, D., Liska, R., & Saltelli, A. (2007). The role of sensitivity analysis in ecological modelling. *Ecological Modelling*, *203*(1–2), 167–182.

Cavaignac, S. (2009). *Les sylvoécorégions (SER) de France métropolitaine. Etude de définition*. Inventaire Forestier National, Nogent-sur-Vernisson.

Charru, M., Seynave, I., Hervé, J. C., Bertrand, R., & Bontemps, J. D. (2017). Recent growth changes in Western european forests are driven by climate warming and structured across tree species climatic habitats. *Annals of Forest Science*, *74*(2), 1–34.

Denardou-Tisserand, A. (2019). *Changements du stock de bois sur pied des forêts françaises: Description, analyse et simulation sur des horizons temporels pluri-décennal (1975–2015) et séculaire à partir des données de l'inventaire forestier national et de statistiques anciennes*. Doctoral dissertation Université de Lorraine.

Dvorkin, D., 2012. lcmix: Layered and chained mixture models. R package version 0.3/r5.

Egnell, G., Laudon, H., & Rosvall, O. (2011). Perspectives on the potential contribution of Swedish forests to renewable energy targets in Europe. *Forests*, *2*(2), 578–589.

European commission. (2018). A sustainable bioeconomy for Europe: Strengthening the connection between economy, society and the environment. https://ec.europa.eu/research/bioeconomy/pdf/ec_bioeconomy_strategy_2018.pdf

FAO. (2005). *Global forest resource assessment update 2005: Terms and definitions* (p. 2004). Forest Resource Assessment Programme.

FAO & UNEP. (2020). *The state of the world's forests 2020: Forests, biodiversity and people*.

Forest Europe. (2015). *Full state of Europe's forests 2015. Ministerial conference on the protection of forests in Europe, Madrid, Spain*.

Fortin, M., Robert, N., & Manso, R. (2016). Uncertainty assessment of large-scale forest growth predictions based on a transition-matrix model in Catalonia. *Annals of Forest Science*, *73*(4), 871–883.

Gregoire, T. G., & Valentine, H. T. (2007). *Sampling strategies for natural resources and the environment*. Chapman and Hall/CRC.

Henttonen, H. M., Nöjd, P., & Mäkinen, H. (2017). Environment-induced growth changes in the Finnish forests during 1971–2010–An analysis based on National Forest Inventory. *Forest Ecology and Management*, *386*, 22–36.

Hervé, J. C., Wurpillot, S., Vidal, C., & Roman-Amat, B. (2014). L'inventaire des ressources forestières en France: Un nouveau regard sur de nouvelles forêts. *Revue Forestière Française*, *66*(3), 247–260.

IGN. (2018). *Un inventaire forestier annuel sur l'ensemble de la France métropolitaine*. https://inventaire-forestier.ign.fr/spip.php?rubrique25

Keenleyside, C., Tucker, G., & McConville, A. (2010). *Farmland abandonment in the EU: An assessment of trends and prospects*. Institute for European Environmental Policy.

Leslie, P. H. (1945). On the use of matrices in certain population mathematics. *Biometrika*, *33*(3), 183–212.

Likens, G. E. (2013). *Biogeochemistry of a forested ecosystem*. Springer Science & Business Media.

Linkevičius, E., Borges, J. G., Doyle, M., Pülzl, H., Nordström, E. M., Vacik, H., Brukas, V., Biber, P., Teder, M., Kaimre, P., & Synek, M. (2019). Linking forest policy issues and decision support tools in Europe. *Forest Policy and Economics*, *103*, 4–16.

Mandallaz, D. (2008). *Sampling techniques for forest inventories*. Chapman and Hall/CRC.

Mather, A. S. (1992). The forest transition. *Area*, *24*(4), 367–379.

McCormick, K., & Kautto, N. (2013). The bioeconomy in Europe: An overview. *Sustainability*, *5*(6), 2589–2608.

McRoberts, R. E., & Lessard, V. C. (2001). Estimating the uncertainty in diameter growth model predictions and its effects on the uncertainty of annual inventory estimates. In Proceedings of the Second Annual Forest Inventory and Analysis (FIA) Symposium (pp. 70–75).

McRoberts, R. E., & Westfall, J. A. (2014). Effects of uncertainty in model predictions of individual tree volume on large area volume estimates. *Forest Science*, *60*(1), 34–42.

Ministry of Ecological Transition. (2020). Stratégie nationale bas-carbone. https://www.ecologie.gouv.fr/strategie-nationale-bas-carbone-snbc

Ols, C., Hervé, J. C., & Bontemps, J. D. (2020). Recent growth trends of conifers across Western Europe are controlled by thermal and water constraints and favored by forest heterogeneity. *Science of the Total Environment*, *742*, 140453.

Pan, Y., Birdsey, R. A., Fang, J., Houghton, R., Kauppi, P. E., Kurz, W. A., Phillips, O. L., Shvidenko, A., Lewis, S. L., Canadell, J. G., & Ciais, P. (2011). A large and persistent carbon sink in the world's forests. *Science*, *333*(6045), 988–993.

Picard, N., Ouédraogo, D., & Bar-Hen, A. (2010). Choosing classes for size projection matrix models. *Ecological Modelling*, *221*(19), 2270–2279.

Pignard, G. (1994). *Estimation des prélèvements de bois dans la forêt française; Approche forestière de l'autoconsommation*. Inventaire forestier national IFN: Agence de l'Environnement et de la Maîtrise de l'Energie Ademe.

Rautiainen, A., Wernick, I., Waggoner, P. E., Ausubel, J. H., & Kauppi, P. E. (2011). A national and international analysis of changing forest density. *PLoS One*, *6*(5), 19577.

Redsven, V., Hirvelä, H., Härkönen, K., Salminen, O., & Siitonen, M. (2013). *MELA2012 reference manual*.

Roux, A., Colin, A., Dhôte, J. F., & Schmitt, B. (2020). *Filière forêt-bois et atténuation du changement* (p. 172). Editions Quae.

Siitonen, M., Härkönen, K., Hirvelä, H., Jämsä, J., Kilpeläinen, H., Salminen, O., & Teuri, M. (1996). *MELA handbook*. Metsäntutkimuslaitos.

Thürig, E., Kaufmann, E., Frisullo, R., & Bugmannc, H. (2005). Evaluation of the growth function of an empirical forest scenario model. *Forest Ecology and Management*, *204*(1), 53–68.

Thürig, E., & Schelhaas, M. J. (2006). Evaluation of a large-scale forest scenario model in heterogeneous forests: A case study for Switzerland. *Canadian Journal of Forest Research*, *36*(3), 671–683.

Tomlin, A. S. (2013). The role of sensitivity and uncertainty analysis in combustion modelling. *Proceedings of the Combustion Institute*, *34*(1), 159–176.

Tomppo, E., Gschwantner, T., Lawrence, M., McRoberts, R. E., Gabler, K., Schadauer, K., Vidal, C., Lanz, A., Ståhl, G., & Cienciala, E. (2010). National forest inventories. Pathways for Common Reporting. *European Science Foundation*, *1*, 541–553.

Usher, M. B. (1966). A matrix approach to the management of renewable resources, with special reference to selection forests. *Journal of Applied Ecology*, *3*, 355–367.

Usher, M. B. (1969). A matrix model for forest management. *Biometrics*, *25*, 309–315.
Van Oijen, M. (2017). Bayesian methods for quantifying and reducing uncertainty and error in forest models. *Current Forestry Reports*, *3*(4), 269–280.
Vanclay, J. K., & Skovsgaard, J. P. (1997). Evaluating forest growth models. *Ecological Modelling*, *98*(1), 1–12.
Vauhkonen, J., Berger, A., Gschwantner, T., Schadauer, K., Lejeune, P., Perin, J., Pitchugin, M., Adolt, R., Zeman, M., Johannsen, V. K., & Kepfer-Rojas, S. (2019). Harmonised projections of future forest resources in Europe. *Annals of Forest Science*, *76*(3), 1–12.
Vauhkonen, J., & Packalen, T. (2018). Uncertainties related to climate change and forest management with implications on climate regulation in Finland. *Ecosystem Services*, *33*, 213–224.
Wernsdörfer, H., Colin, A., Bontemps, J. D., Chevalier, H., Pignard, G., Caurla, S., Leban, J. M., Hervé, J. C., & Fournier, M. (2012). Large-scale dynamics of a heterogeneous forest resource are driven jointly by geographically varying growth conditions, tree species composition and stand structure. *Annals of Forest Science*, *69*(7), 829–844.
Westfall, J. A., & Patterson, P. L. (2007). Measurement variability error for estimates of volume change. *Canadian Journal of Forest Research*, *37*(11), 2201–2210.
Zhu, Y., Hogan, J. A., Cai, H., Xun, Y., Jiang, F., & Jin, G. (2017). Biotic and abiotic drivers of the tree growth and mortality trade-off in an old-growth temperate forest. *Forest Ecology and Management*, *404*, 354–360.

SUPPORTING INFORMATION

Additional supporting information can be found online in the Supporting Information section at the end of this article.

How to cite this article: Audinot, T., Wernsdörfer, H., Le Moguédec, G., & Bontemps, J.-D. (2022). Modeling and propagating inventory-based sampling uncertainty in the large-scale forest demographic model "MARGOT". *Natural Resource Modeling*, 35, e12352. https://doi.org/10.1111/nrm.12352